

## Supplementary Materials for

### Engineering entropy for the inverse design of colloidal crystals from hard shapes

Yina Geng, Greg van Anders\*, Paul M. Dodd, Julia Dshemuchadse, Sharon C. Glotzer\*

\*Corresponding author. Email: [gva@queensu.ca](mailto:gva@queensu.ca) (G.v.A.); [sglotzer@umich.edu](mailto:sglotzer@umich.edu) (S.C.G.)

Published 5 July 2019, *Sci. Adv.* **5**, eaaw0514 (2019)

DOI: 10.1126/sciadv.aaw0514

#### The PDF file includes:

- Symmetric shape constructions
- Demonstration of successful self-assembly
- Direct free energy computation
- Table S1. Mean of cosine of dihedral angle distribution.
- Table S2. Optimal geometric parameters.
- Fig. S1. Symmetric shape families.
- Fig. S2. Successful self-assembly from disordered fluid.
- References (46–48)

#### Other Supplementary Material for this manuscript includes the following:

(available at [advances.sciencemag.org/cgi/content/full/5/7/eaaw0514/DC1](https://advances.sciencemag.org/cgi/content/full/5/7/eaaw0514/DC1))

Movie S1 (.mp4 format). Alch-MC and regular MC for the  $\beta$ -Mn structure.

## Symmetric shape constructions

We describe the construction of symmetric shape families for inverse engineering optimal particle shapes for each candidate structure. In all cases, after the geometric construction below was carried out, all particle shapes were normalized to unit volume to maintain constant system density.

### BCC and FCC

We focus on the spheric triangle group  $\Delta_{4,3,2}$  [45], which is constructed with three families of planes that make up the faces of a rhombic dodecahedron, a cube, and an octahedron. There are truncating planes of two types: type *a* corresponding to the location of the cube faces, and type *c* which correspond to the position of the octahedron faces. We use  $\alpha$  to represent the location of the truncating planes of type *a* and  $\beta$  to represent the location of the truncating planes of type *c*, both of which are linearly mapped to the interval between 0 and 1. (0, 0) is the cuboctahedron, (0, 1) is the cube, (1, 0) is the octahedron and (1, 1) is the rhombic dodecahedron. For a detailed mathematical construction and images of representative particle shapes see Ref. [45].

### $\beta$ -Mn

We truncate each vertex of a dodecahedron using planes with normals directed along a line connecting the geometric center of the dodecahedron with a vertex, truncating by an amount  $\alpha$  between 0 and 1. The perfect dodecahedron has  $\alpha = 1$ , and  $\alpha = 0$  when two truncating vertices meet. Representative particles from this shape family are shown in fig. S1B.

### SC

We first study the spheric triangle group  $\Delta_{3,2,3}$  [45] which is constructed with three families of planes that make up the faces of a cube, a tetrahedron, and an octahedron. As in the case of the  $\Delta_{4,3,2}$  family, there are two shape parameters, *a* and *c*, which specify the amount of truncation (or position of the bounding planes). For a detailed mathematical construction and images of representative particle shapes see Ref. [46].

We then study a one-parameter family of shapes formed by adding a vertex at each face center of a cube. Shape parameter  $\alpha = 0$  describes a perfect cube and  $\alpha = 1$  describes a perfect rhombic dodecahedron. Representative particles from this shape family are shown in fig. S1A.

### Diamond

We first study a one-parameter truncated tetrahedron family, where we truncate each vertex of a tetrahedron by an amount  $\alpha$  that ranges between a perfect tetrahedron ( $\alpha = 1$ ) and an octahedron ( $\alpha = 0$ ). Representative particles from this shape family are shown in fig. S1C (top).

We then study a three-parameter shape family formed by truncating the vertices of a tetrahedron and adding one more vertex to each face. Each augmenting vertex lies along a line connecting the geometric center of the tetrahedron with the center of a face. For this shape family, we again use  $\alpha$  to parametrize the amount of truncation on each vertex of the tetrahedron. For the hexagonal faces of a truncated tetrahedron, we use shape parameter  $\beta$  to measure the distance between the augmenting vertex on the tetrahedron face and the

original face center. We use  $\beta = 0$  to indicate that the augmenting vertex lies in the plane of the tetrahedron face (*i.e.* no augmentation), and  $\beta = 1$  to indicate that the distance between the augmenting vertex and center of mass (CM) is twice the distance between the original face center and CM. For the triangular faces of the truncated tetrahedron, we use shape parameter  $\gamma$  to measure the distance between the augmenting vertex and CM. We use  $\gamma = 0$  to indicate that the location of the augmenting vertex coincides with the vertex location of a regular (*i.e.* untruncated) tetrahedron and  $\gamma = 1$  to indicate that the augmenting vertex lies at the CM. Representative particles from this shape family are shown in fig. S1C (bottom).

### $\beta$ -W

We first study a two-parameter family of asymmetrically truncated dodecahedral shapes. We divide the vertices of a dodecahedron into two groups of ten, with one group of vertices on the two parallel faces. Taking the convex hull of the remaining “side” vertices yields a pentagonal antiprism, with pentagonal faces parallel to the top and bottom faces of the dodecahedron. We use  $\alpha$  to parametrize the truncation of vertices on the top and bottom faces by truncating planes that lie parallel to the top and bottom faces and are equidistant to the particle CM. We use  $\alpha = 1$  to indicate that the truncating planes are coplanar with the top and bottom faces of the dodecahedron, and we use  $\alpha = 0$  to indicate the truncating planes lie halfway between the top and bottom faces and the pentagonal faces of the antiprism. We use  $\beta$  to parametrize the truncation of the side vertices. The truncations are formed by situating ten equidistant planes that have face normals parallel to directions passing through the particle CM and each side vertex. We use  $\beta = 1$  to indicate no vertex truncation and  $\beta = 0$  for the case when two truncated vertices meet. Representative particles from this shape family are shown in fig. S1E (top).

We then study a four-parameter shape family with two parameters describing the vertex truncations as indicated above. The other two parameters describe vertex augmentation. We use  $\gamma$  to parametrize vertex augmentation of the side faces. We use  $\gamma = 0$  to indicate that the augmenting vertex lies in the plane of the face (*i.e.* no vertex augmentation) and  $\gamma = 1$  to indicate the distance between the augmenting vertex and CM is twice the distance between original face center and CM. We use  $\delta$  to parametrize the position of the vertices that augment the top and bottom faces along lines connecting the center of the particle with the centers of the top and bottom faces. We use  $\delta = 0$  to indicate that the augmenting vertex lies at the initial pentagon face center and  $\delta = 1$  to indicate the augmenting vertex is at the CM. Representative particles from this shape family are shown in fig. S1E (bottom).

### hP2-X

This hypothetical structure is a derivative of the hexagonally close-packed structure (HCP). The structures are very similar from a crystallographic viewpoint: both exhibit space group  $P6_3/mmc$  (space group no. 194) and in both of them, the same Wyckoff site is occupied:  $2c$   $1/3, 2/3, 1/4$ . However, the ratio of unit cell parameters  $c/a$  differs substantially between these two cases. While for the close-packing of spheres

$c/a = \sqrt{8/3} \approx 1.633$ , this is a free parameter from a symmetry point of view. For the structure used here, we chose a much lower value of  $c/a = 0.639$ .

This variant of the crystallographically identical unit cell exhibits a different local particle environment, due to the fact that particles can move closer together along the  $c$ -direction and therefore are farther apart, relatively, in the  $a$ - $b$ -plane. This leads to a coordination number of 8 nearest neighbors – compared with 12 in HCP – and a coordination polyhedron with the shape of a biaugmented triangular prism.

We first study a two-parameter family of asymmetrically truncated bipyramid shapes. The dihedral angle between the upper and lower face of the bipyramid is 122.049 degrees. We divide the vertices of a bipyramid into two groups, with one group of vertices at the top and bottom, and another group of three vertices on the side. We use  $\alpha$  to parametrize the truncation of the top and bottom vertices. We use  $\alpha = 1$  to indicate no vertex truncation, and  $\alpha = 0$  to indicate the vertices are truncated to the side vertex position. We use  $\beta$  to parametrize the truncation of the side vertices. The truncations are formed by situating three equidistant planes that have face normals parallel with passing through the particle CM and each side vertex. We use  $\beta = 1$  to indicate no vertex truncation and  $\beta = 0$  for the case when two truncated vertices meet. Representative particles from this shape family are shown in fig. S1D (left).

We then study a four-parameter shape family with two parameters describing the vertex truncations as indicated above. The other two parameters describe vertex augmentation. We use  $\gamma$  to parametrize the position of the vertices that augment the top and bottom faces along directions connecting the center of the particle with the top and bottom vertices. We use  $\gamma = 0$  to indicate that the augmenting vertex lies at the initial top and bottom vertices and  $\gamma = 1$  to indicate the augmenting vertex is at the particle CM. We use  $\delta$  to parametrize vertex augmentation of the side faces. We chose the augmenting vertex to be the side face center of a shape with  $\alpha = 0.435, \beta = 0.52, \gamma = 0.503$ . We use  $\delta = 0$  to indicate that the augmenting vertex lies in the plane of the face (*i.e.* no vertex augmentation) and  $\delta = 1$  to indicate the distance between the augmenting vertex and CM is twice the distance between the original augmenting vertex and CM. Representative particles from this shape family are shown in fig. S1D (right).

### Demonstration of successful self-assembly

For the structures BCC, FCC,  $\beta$ -Mn, SC, diamond, and  $\beta$ -W, we confirmed the successful self-assembly of each target structure using a geometric ansatz where particles have the shape of the Voronoi cell of the target crystal structure, a near optimal unsymmetrized shape from Alch-MC simulation, and the symmetric optimal shape from Alch-MC simulation (see fig. S2 for representative system snapshots). Self-assembly validation was performed using the Hard Particle Monte Carlo (HPMC) [38] plugin for HOOMD-blue [40]. We simulated in the  $NVT$  ensemble with 2197 particles for all structures at packing fraction  $\eta = 0.6$ , with between  $4 \times 10^7$  and a maximum of  $1 \times 10^9$  Monte Carlo sweeps. We identified an as-

sembled crystal structure by computing bond order diagrams and diffraction patterns using particle centroids, following the approach used in Ref. [11].

### Direct free energy computation

We computed the Helmholtz free energy difference between the target crystal and the Einstein crystal using Frenkel-Ladd thermodynamic integration [43] *via* the implementation used in Refs. [38, 47]. We placed approximately 2000 particles in a periodic simulation box; the exact number was chosen to be a multiple of the number of particles in the unit cell of the target structure. For SC, BCC, diamond, and  $hP2$ -X structures, particles in the assembled structure have orientational order. Einstein crystal positions and orientations were taken directly from the space-filling tessellation. For FCC,  $\beta$ -W, and  $\beta$ -Mn structures, particles in the assembled structure do not show orientational order. To create an appropriate Einstein crystal, we first initialized the simulation at a low packing fraction  $\eta = 0.5$ , chose particle positions using the target structure, and randomly assigned a set of orientations observed in the assembly. Then we compressed the system to packing fraction  $\eta = 0.6$ , allowing particles to rotate to resolve overlaps. We computed the alchemical free energy of the target structure [14]. We normalized free energies in all plots by setting the free energy of the target structure with the Voronoi particles to be zero. Negative values of the free energy indicate lower free energy for a given particle than a Voronoi particle shape.

We validated our methodology by performing the free energy calculation described above for truncated tetrahedra in a diamond structure, and checked that it reproduces the results reported in Ref. [14] computed *via* the Bennett acceptance ratio method [48].

**Table S1. Mean of cosine of dihedral angle distribution.** Mean of cosine of dihedral angle distribution for unsymmetrized optimal shapes in step one for seven target structures, which used to infer symmetry-restricted shapes in step two.

Structure	mean of cosine of dihedral angle distribution			
BCC	-1/3	1/3	1	N/A
FCC	-1/2	0	1/2	1
$\beta$ -Mn	-0.447	0.447	1	N/A
SC	0	1	N/A	N/A
Diamond	1/3	N/A	N/A	N/A
$\beta$ -W	-0.447	0.447	1	N/A
<i>hP2-X</i>	-0.531	-0.484	0.148	0.617

**Table S2. Optimal geometric parameters.** Optimal geometric parameters (see Symmetric Shape Constructions section for parameter descriptions) from Alch-MC simulation for symmetric convex polyhedra in step two to self-assemble seven target structures.

Structure	$\alpha$	$\beta$	$\gamma$	$\delta$
BCC	0.476	0.194	N/A	N/A
FCC	0.341	0.318	N/A	N/A
$\beta$ -Mn	0.263	N/A	N/A	N/A
SC	0.130	N/A	N/A	N/A
Diamond	0.392	0.111	0.350	N/A
$\beta$ -W	0.564	0.486	0.122	0.081
<i>hP2-X</i>	0.451	0.608	0.487	0.043



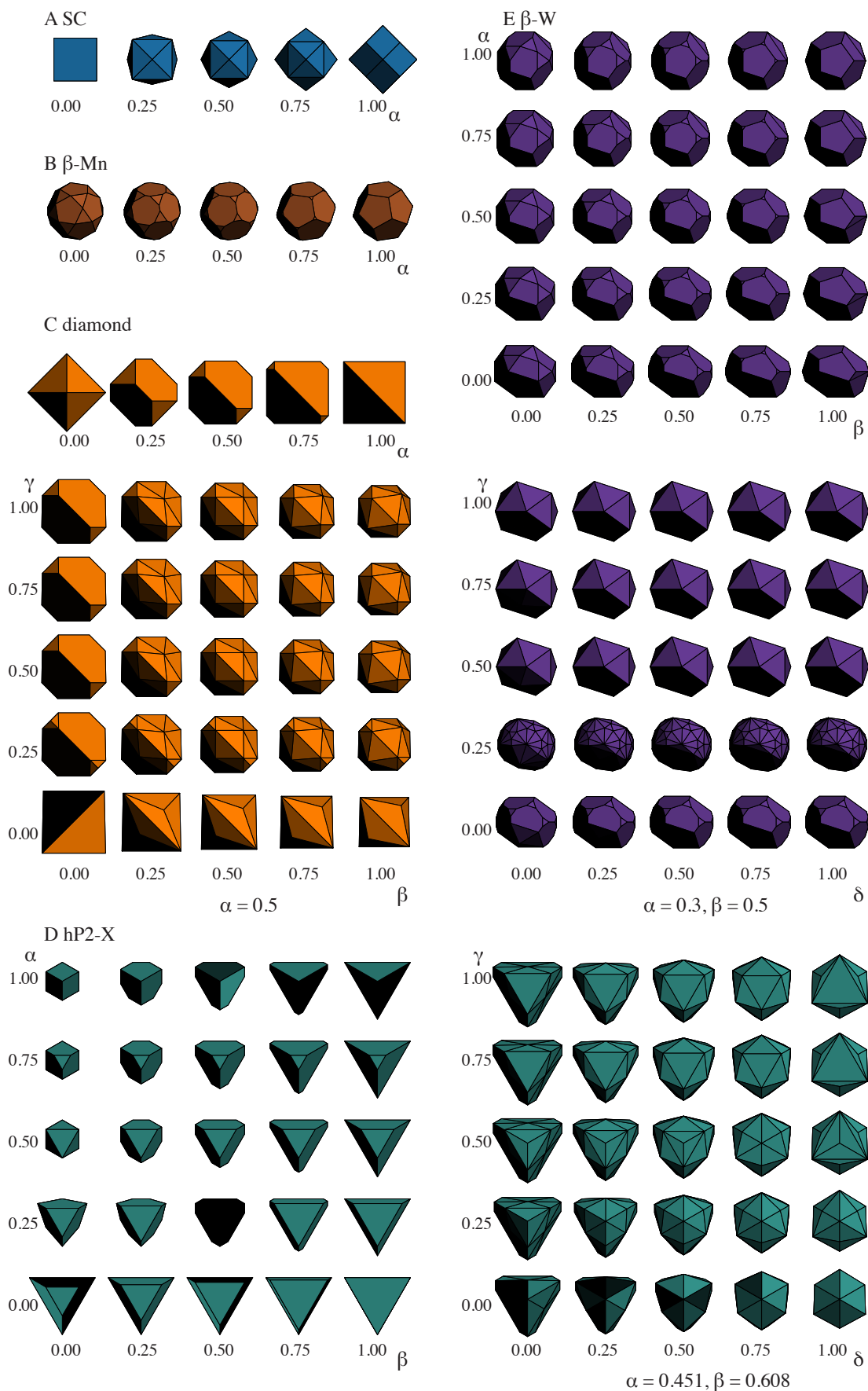


Fig. S1. **Symmetric shape families.** Illustration of the geometric constructions used to create symmetric, convex polyhedra for the target structures: SC,  $\beta$ -Mn, diamond,  $\beta$ -W, and hP2-X in step two. See Symmetric Shape Constructions section for a detailed description.

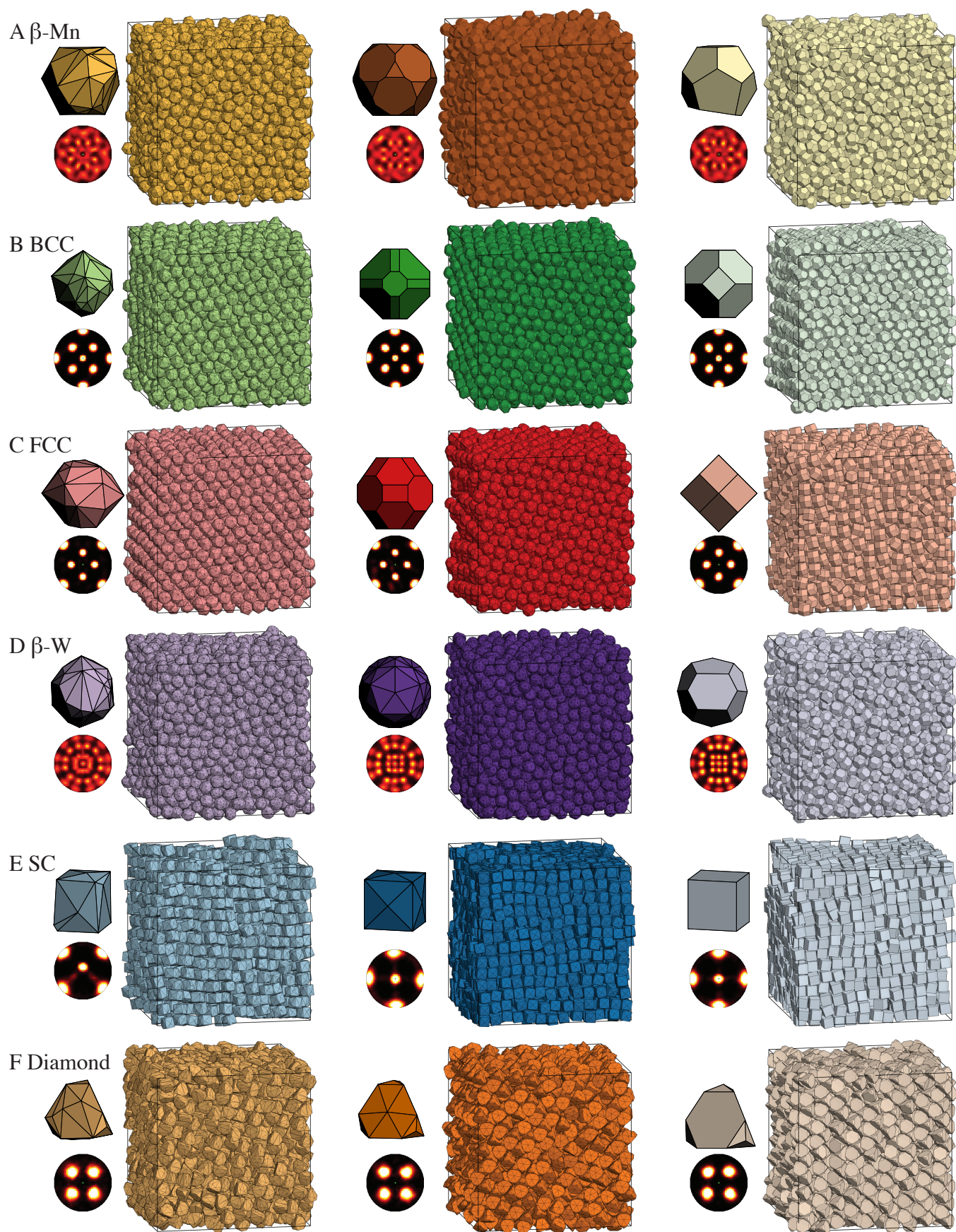


Fig. S2. **Successful self-assembly from disordered fluid.** Representative system snapshots indicating the successful self-assembly in *NVT* MC simulations of near-optimal convex polyhedra obtained from Alch-MC simulation in step one (left column), *NVT* MC simulation of optimal symmetric convex polyhedra obtained from Alch-MC simulation in step two (center column), and geometric ansatz (right column) for six structures at packing fraction  $\eta = 0.6$ . Particle images and bond-order diagrams are on the left. (A snapshot of a representative system that successfully self-assembled the *hP2-X* structure is shown in Fig. 3C.)